Hearing Research 464 (2025) 109324

Contents lists available at ScienceDirect

Hearing Research

journal homepage: www.elsevier.com/locate/heares

Contribution of the reticular lamina motion to the traveling wave: a WKB approach

Renata Sisto [a], Arturo Moleti [b,*]

[a] Department of Occupational and Environmental Medicine, Epidemiology and Hygiene, INAIL-National Research Centre for Safety and Prevention at Workplace, Monteporzio Catone(Rome), Italy
[b] Department of Physics and NAST Center, University of Rome 'Tor Vergata', Rome, Italy

ARTICLE INFO

Keywords:
Cochlear modeling
Traveling waves
WKB approximation
Organ of corti

ABSTRACT

Optical coherence tomography (OCT) experiments showed that, in the peak region, at low stimulus levels, the motion of the reticular lamina (RL) may be larger than that of the basilar membrane (BM), suggesting that the contribution of the RL motion to the development of a slow traveling wave (TW) could be a relevant one. In this study, a transmission-line cochlear model with two mechanical degrees of freedom at each tonotopic place is used, in which the outer hair cell (OHC) force is represented by a low-pass filtered elastic term proportional to the OHC elongation. The hydrodynamic effects of fluid focusing and viscous damping in the peak region are also included in the model. In the simulations, the contribution of the RL motion to the traveling wave is due to the volume change of the Organ of Corti (OoC), which adds up to the antisymmetric volume change of the two scalae associated with the BM motion. Including the RL motion in the computation of the local wavenumber in the Wentzel-Kramers-Brillouin (WKB) framework implies a change of both the focusing factor and of the real part of the admittance, dependent on the phase of the relative RL-BM motion. To make the RL contribution on focusing the most effective, the BM and the RL should be approximately in phase in the peak region, which, in the model, is consistent with a dominant gain effect of fluid focusing over OHC internal force in the peak region. The negative/positive sign of the RL-BM local phase shift would imply an additional damping/antidamping effect, which is more difficult to predict, and model-dependent.

1. Introduction

Recent optical coherence tomography (OCT) experiments (e.g., (Cho and Puria, 2022; Cooper et al., 2018; He et al., 2022; Lee et al., 2016; Strimbu et al., 2024), recently reviewed in (Olson et al., 2025)) studied the motion of the basilar membrane (BM) and of the reticular lamina (RL) in correspondence of each outer hair cell (OHC) row (Cho and Puria, 2022), as well as the motion of the junction between the OHC body and the Deiter's cells. Over a wide cochlear region basal to the peak, at low stimulus levels, the motion of the RL is significantly larger than that of the BM. This circumstance inspired an "overturned view" (Altoè et al., 2022) of the OHCs cochlear amplification mechanism. According to this view, the most important structure for the development and amplification of the traveling wave (TW) in the peak region would be the upper part of the Organ of Corti (OoC), which moves more than the BM, causing therefore the main volume deformation in the upper fluid chamber. Indeed, the TW transmission is due to the interplay between the motion of the elements of the OoC and the fluid incompressibility: the volume change of the fluid filled chambers produces a longitudinal velocity gradient, whose time derivative is related by the Navier-Stokes equations (neglecting viscosity) to the spatial second derivative of the differential pressure. This way, a propagation equation is obtained for the TW, and the resulting wavenumber is a function of the local admittance. In the traditional view of the OHCs amplification mechanism, even in two-degrees-of-freedom (2DOF) models that account for the motion of different parts of the OoC (Neely and Kim, 1986; Sisto et al., 2019), only the coupling of the BM motion to the dynamics of the incompressible fluid is responsible for the development of the TW. In the overturned view, the OHCs elongation mainly produces an area deformation in the upper part of the OoC, causing a large longitudinal gradient of the vertical velocity in the fluid volume located above. In any case, both the BM and the RL velocities could contribute to the TW complex wavenumber and, in the peak region, the RL contribution could be the most relevant one, whereas in the long-wave region the main

* Corresponding author.
E-mail addresses: r.sisto@inail.it (R. Sisto), moleti@roma2.infn.it (A. Moleti).

https://doi.org/10.1016/j.heares.2025.109324
Received 11 December 2024; Received in revised form 11 May 2025; Accepted 27 May 2025
Available online 5 June 2025

contribution to the development of the TW would still be given by the BM motion.

Another aspect of the overturned view is related to the energy transfer between the OHC and the different elements of the OoC. Due to the large estimated compliance of the Deiter's cells (Zhou et al., 2022) it was argued that the OHCs could not effectively transfer mechanical energy to the BM (Altoè et al., 2022), unless one assumes a different pathway for mechanical power transfer to the BM. In (Samaras and Meaud, 2024), Samaras and coworkers showed that such an alternative pathway may be present, involving the very stiff pillar cells. The controversy about whether positive mechanical work of the OHCs could directly be done on the BM is largely decoupled from the topic of the present paper, i.e., that the motion of the upper part of the OoC should be kept into account in any case in TW generation modeling, particularly in the short-wave region.

Constraints to such TW generation models are imposed by experimental measurements of the RL-BM relative phase. Realistic cochlear models should match the common properties of the experimental observations. OCT data are available but there is still some uncertainty about the RL-BM difference, mainly due to the effect the optical axis inclination (Olson et al., 2025) and to the presence of large longitudinal and radial components of the OoC motion (Cho and Puria, 2022; Cooper et al., 2018). In these experiments, a monotonic decrease of the RL-BM phase difference is generally observed with increasing frequency, and, in the peak region, small phase differences, generally negative, or slightly positive, are reported (Cho and Puria, 2022; Cooper et al., 2018; He et al., 2022; Lee et al., 2016; Strimbu et al., 2024). Given this variability, in this study we will tune the model parameters in order to get a small RL-BM phase difference, between 0 and $-90°$, and we will discuss the effect of small positive and negative phase differences, which cannot be ruled out, to our knowledge, by the observations.

In this study, a transmission-line 2DOF cochlear model is solved in the Wentzel-Kramers-Brillouin (WKB) approximation. The WKB method has been extensively used (see, e.g., (Steele and Taber, 1979; Zweig, 1991; Frost BL 2024; Shera et al., 2005)) to find analytical solutions of the linearized cochlear equations that provide deep physical insight into the transmission, absorption and reflection properties of the cochlea. The two mechanical elements that schematically represent the complexity of the OoC are associated here with the BM and the RL. The OHC internal force acting between the two masses is represented by a low-pass filtered elastic term proportional to the OHC elongation. With respect to previous 1-D studies (e.g., (Neely and Kim, 1986)), this model also includes the fluid focusing effect and the viscous damping effect in the peak region. A set of linear models with different effectiveness of the OHC mechanism is used to roughly represent the nonlinear response of the cochlea to different stimulus levels. We add the RL contribution to the TW wavenumber, assuming that a single transmission equation still holds with separate contributions to the second derivative of the pressure (and therefore to the complex wavenumber squared) coming from the motion of the BM (yielding velocity gradients in both scalae) and of the RL (acting on the tympanic scala only). A modified relation between the wavenumber and the local BM admittance is obtained keeping into account also the 2-D hydrodynamic effects (pressure focusing and viscous losses) that are very relevant in the short-wave region.

We discuss the relative phase conditions for the RL and BM that boost the pressure focusing effect and their effect on the amplification of the TW by the active force. While the first effect is easily predictable (maximal boost for in-phase BM and RL motion), we will see that, for active models, the damping/anti-damping effect on the imaginary part of the wavenumber may be sensitive to small changes of the relative RL-BM phase.

2. Model

In a recent 2DOF 1-D transmission line cochlear model (Sisto et al., 2019), the local mechanical element consisted of two oscillators, with masses $M_1 >> M_2$. The two masses were identified, respectively, with the basilar membrane (BM) and the reticular lamina (RL), coupled by the internal active nonlinear OHC force. The OHC mechanism is activated by the relative RL-TM shear motion. In the model, this motion was simply schematized as proportional to the OHC elongation, or the relative RL-BM displacement. Thus, the input to the electromotility of the OHC system was represented by an instantaneous nonlinear function of the local relative RL-BM displacement.

The model predicted the observed nonlinearity of the RL response over a large basal region, and respected quite naturally the zero-crossing intensity invariance of the impulse response (Shera, 2001). The main drawbacks of that model were:

1) an insufficiently physiologically-based representation of the OHC micromechanics, in particular having neglected the low-pass characteristic of the electrical response of the OHCs (Samaras and Meaud, 2024);
2) having neglected 2-D, 3-D fluid phenomena that enhance the fluid pressure near the BM (pressure focusing), significantly boosting the cochlear gain though pressure amplification, without the need for a peaked admittance;
3) having neglected the viscous damping associated with the development of sharp vertical velocity gradients in the peak region at the fluid-BM boundary.

In the present model (see (Sisto and Moleti, 2021; Sisto et al., 2021; Sisto et al., 2023)), within the limits of the linear WKB approximation, these issues were addressed by introducing:

1) a more physiologically-based model of the OHC mechanism, proposed by Lu et al. (Lu et al., 2006), including the low-pass behaviour associated with the slow build-up of the OHC transmembrane potential.
2) an estimate, following Duifhuis and Shera (Shera et al., 2005; Duifhuis, 2012), of the 2-D pressure focusing effect on the BM gain, dependent of the local growth of the wavenumber in the short-wave region, was introduced.
3) a vector potential formulation of the cochlear fluid mechanics, used, following Steele and coworkers (Steele and Taber, 1979; Wang et al., 2016), to schematize the viscous force exerted by the fluid on the BM.

The linearized equations of motion for the system of coupled oscillators are written in the frequency domain as:

$$\begin{cases} Z_1\dot{\xi}_1 + Z_3(\dot{\xi}_1 - \dot{\xi}_2) + Z_{\mathrm{OHC}}(\dot{\xi}_1 - \dot{\xi}_2) = p \\ Z_2\dot{\xi}_2 - Z_3(\dot{\xi}_1 - \dot{\xi}_2) - Z_{\mathrm{OHC}}(\dot{\xi}_1 - \dot{\xi}_2) = 0 \end{cases} \quad (1)$$

where a hybrid notation is used, with $\dot{\xi}_{1,2}$ meaning the Fourier Transform of the velocity. p is the differential pressure acting at $z = 0$ on the BM only, and all functions depend on frequency ω and longitudinal position x.

Equations (1) are graphically represented by the diagram in Fig. 1:

The impedances of the linear oscillators of mass M_1 and M_2, damping coefficient C_1 and C_2, and stiffness K_1 and K_2, can be written as:

$$Z_{1,2} = sM_{1,2} + C_{1,2} + \frac{K_{1,2}}{s}, \quad (2)$$

with $s = i\omega$. The impedance associated with a passive interaction term between the two is:

$$Z_3 = C_3 + \frac{K_3}{s}. \quad (3)$$

The active force term is written as an internal force, triggered by a current proportional to the OHC elongation. The low-pass filtering effect of the slow build-up of the transmembrane potential that yields the active force, and the viscous fluid damping effect on the BM motion are

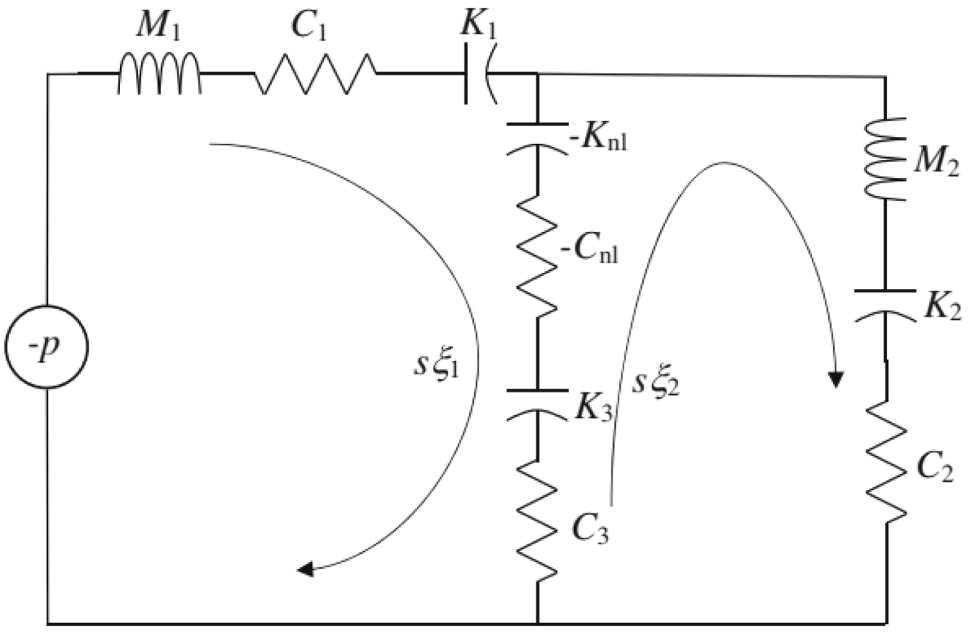

Fig. 1. Circuital representation of the system of equations (1). The internal nonlinear OHC force between BM and RL is represented by the K_{nl} and C_{nl} lumped elements.

also kept into account. The local cut-off frequency of the OHC low-pass filter can be set according with physiological data (Nam and Fettiplace, 2012), which show a strong spatial dependence of membrane conductance and capacitance. The low-pass frequency of the filter monotonically changes along the BM, as the CF, but with a slightly slower spatial gradient. As a consequence, the local characteristic frequency is close to the local cut-off frequency in the apical end of the BM, and well above it in the basal cochlea.

For frequencies above the local cut-off frequency, two competing effects occur (Sisto and Moleti, 2021):

1) the output amplitude is attenuated by the filter response with a 6 dB/oct slope,
2) the up-to-90° phase shift of the OHC active term (here schematized as a combination of elastic and damping terms) yields effective anti-damping action, compensating for the increase of viscous losses in the local admittance, within a wide region basal to the nominal resonant place, where the wavenumber is still approximately real.

The active force on the BM may be written in the frequency domain as:

$$F_{OHC} = Z_{OHC}(\dot{\xi}_2 - \dot{\xi}_1), \tag{4}$$

The impedance of the OHC term, including the low-pass effect on amplitude and phase associated with the characteristic time $\tau(x)$, is:

$$Z_{OHC} = G\left(C_{nl} + \frac{K_{nl}}{s}\right)\frac{1}{(1+s\tau)}. \tag{5}$$

where G, variable between 0 and 1, is a parameter controlling the strength of the active force, roughly describing the nonlinear behavior of the response at different stimulus levels. Here, for simplicity, we assume $C_{nl} = 0$. Similarly to (Wang et al., 2016), the nonlinear dependence of the active force on the instantaneous displacement was roughly schematized by solving a set of linear models with different strengths of the OHC active term.

Starting from the system of Eq. (1), the BM admittance can be easily calculated:

$$Y_1 = \frac{Z_2 + Z_3 + Z_{OHC}}{Z_1 Z_2 + (Z_{OHC} + Z_3)(Z_1 + Z_2)}. \tag{6}$$

The complex ratio between the RL and the BM velocity is:

$$\frac{\dot{\xi}_2}{\dot{\xi}_1} = \frac{Z_3 + Z_{OHC}}{(Z_2 + Z_3 + Z_{OHC})}. \tag{7}$$

Eq. (7) suggests that the model parameters can be set such that the ratio is larger than unity or, in other words, the RL moves more than BM at low stimulus levels, i.e., in the linearized solution, for the maximal strength of the active term. This condition can be obtained by setting $Z_{OHC} \sim -(Z_2 + Z_3)$ in the large gain limit, so Eq. (7) tends to a value approaching or exceeding unity.

Due to the fluid incompressibility, the transverse displacement of the OoC structures develops longitudinal gradients of the fluid longitudinal velocity. The time derivative of the velocity gradient, neglecting viscosity in the Navier-Stokes equations, is proportional to the spatial second derivative of the differential pressure, yielding the equation describing the TW propagation. In the 1-D (long-wave approximation, fluid variables independent of the vertical coordinate z), 1DOF (OoC consisting of the BM only) case, the propagation equation for the TW is written in the frequency domain as:

$$\frac{\partial^2 p}{\partial x^2} = 2i\omega\frac{\rho}{H}\dot{\xi}_1 = 2i\omega\frac{\rho}{H}Y_1 p = -k^2 p, \tag{8}$$

where H is the height of the SV and ST, assumed here to be constant.

The 2-D hydrodynamics permits to keep into account (Sisto et al., 2021):

1) The fluid focusing effect or, in other words, the boost given to the pressure by the shape factor deriving from the short-wave effect.
2) The stabilizing effect deriving from the viscosity or, in other words, the damping term proportional to the wave vector amplitude coming from the viscous friction force acting on the BM in the vertical direction.

In a 2-D model, the forward WKB solution for the pressure field is given by:

$$p(\omega,x,z)=p_0 f(\omega,x)\cosh(-kz)e^{-i\int_0^x k(\omega,x)dx}, \quad (9)$$

where the 2-D expression for $f(\omega,x)$ is a function (see (Duifhuis, 2012)) that in the long-wave 1-D limit is well approximated by $\sqrt{\frac{k(\omega,0)}{k(\omega,x)}}$, while in the short-wave limit it tends to a constant value: $\sqrt{2k(\omega,0)H}$. Here we neglect the separation between the Scala Media (SM) and the Scala Vestibuli (SV), because they are separated by a compliant Reissner membrane (RM), so we assume that the vertical dependence of the hydrodynamic variables, pressure and velocity, is described by a single continuous exponential function ignoring the separation between endolymph and perilymph.

In 2-D models, a propagation equation is obtained for the pressure averaged over the vertical direction [Shera, Sisto]. The fluid focusing effect is kept into account by the factor α representing the ratio between the pressure at the fluid-membrane interface (which is the one related by the BM admittance to the BM velocity) and the pressure averaged over the vertical direction z (Shera et al., 2005; Sisto et al., 2021):

$$\bar{p}(\omega,x)=\frac{p(\omega,x,z=0)}{\alpha}, \quad \text{with } \alpha=\frac{kH}{\tanh(kH)} \quad (10)$$

$$\frac{\partial^2\bar{p}}{\partial x^2}=2i\frac{\omega\rho}{H}Y_1\alpha\bar{p}=-k^2\bar{p} \quad (11)$$

The wavenumber of the 2-D TW obeys therefore the relation:

$$k^2=2i\frac{\omega\rho}{H}\alpha Y_1 \quad (12)$$

This equation yields a smoothly varying wavenumber function that connects in a continuous way the solutions valid in the long- and short-wave approximations.

In 2DOF models, both the BM and the RL contributions to the development of the TW should be considered. The TW generation is due to both the BM displacement and to the OoC section area deformation occurring in the upper part of the OoC. The total OoC section area deformation associated with to the OHC elongation, due to the fluid incompressibility, causes a longitudinal fluid velocity gradient. When the RL moves more than the BM its contributions to the wave vector of the TW can be larger than that of the BM. As in the 1-D case, the incompressibility of the fluid provides the connection between the velocities of the OoC vibrating elements and the differential pressure on the BM, which is also related to the BM velocity by the local admittance function, yielding a closed transmission equation.

In this study, the above described procedure is modified to include the effect of the RL motion on the determination of the wavenumber function:

$$\frac{\partial^2\bar{p}}{\partial x^2}=2i\frac{\omega\rho}{H}(1+\delta)\alpha Y_1\bar{p}=-k^2\bar{p} \quad (13)$$

where the RL relative contribution to the development of a longitudinal velocity gradient, and, consequently, to the wavenumber squared is $\delta=g\frac{\xi_2}{\xi_1}$. The parameter $g<1$ depends on the geometry and may vary across species:

$$g=\frac{1}{2}\frac{w_2}{w_1} \quad (14)$$

where the ratio between the different radial widths of the BM and RL is considered. The factor one-half comes from the fact that the effect of the BM motion is applied coherently to both fluid chambers, while the additional fluid volume change induced by the RL motion asymmetrically affects only the "upper" side.

The contribution to the BM impedance of the viscous force, proportional to the local wavenumber, can be computed following the iterative strategy of the type proposed in (Frost BL 2024; Shera et al., 2005; Sisto et al., 2021; Sisto et al., 2023), using the WKB approximation for solving a model with a 2-,3-D fluid and the linearized 2DOF mechanics described by Eq. (1). An iterative procedure was implemented in (Sisto et al., 2021) to find self-consistent solutions for the wavenumber, starting from the long-wave approximation, and adding the short-wave focusing factor and the viscous damping, both dependent on the wavenumber, until convergence is reached to a self-consistent wavenumber function, valid for a 2-D viscous model.

At the first iteration one computes the wavenumber in the long-wave approximation using the BM admittance Y_{10}, without viscous damping corrections, including also the contribution to the wavenumber associated with the RL motion:

$$k_1^2=-2i\frac{\omega\rho}{H}(1+\delta)Y_{10} \quad (15)$$

In the following iteration, the 2-D approximation is used to get a revised short-wave estimate of the wavenumber:

$$k_2=-2i\frac{\omega\rho}{\tanh(k_1H)}(1+\delta)Y_{10} \quad (16)$$

Then, the full admittance Y_{1V}, is computed adding a viscous damping term to the BM impedance, proportional to real part of the wavenumber:

$$Z_{1V}=Z_1+\frac{4\mu_b}{M_1}Re(k_2) \quad (17)$$

where μ_b is the viscosity coefficient.

In the next iteration, the wavenumber is computed again and used to get a revised 2-d-viscous estimate:

$$k_3=-2i\frac{\omega\rho}{\tanh(k_2H)}(1+\delta)Y_{1V} \quad (18)$$

For $n>3$, the procedure continues iteratively:

$$k_n=-2i\frac{\omega\rho}{\tanh(k_{n-1}H)}(1+\delta)Y_{1V} \quad (19)$$

until convergence is reached.

In Table 1 the model parameters are reported. Here, they are chosen to get a small RL-BM relative phase in the peak region, with no specific reference to any particular experiment, but in reasonable agreement with (Cho and Puria, 2022; Cooper et al., 2018; He et al., 2022; Lee et al., 2016; Strimbu et al., 2024; Olson et al., 2025), meaning only that the RL-BM phase difference is closer to in-phase than to phase opposition. As we just wish to show how the RL motion effect on the TW may be computed in the WKB approximation, the model is not tuned to represent any specific laboratory animal, but the most relevant parameters (e.

Table 1
Cochlear model parameters.

L	Cochlear length	30 [mm]
H	Cochlear duct height	3.5 [mm]
k_ω	Inverse scale length of the cochlear map	200 [m^{-1}]
μ_b	Viscous damping coefficient	2.1 10^{-3} [Pa·s]
M_1	BM surface mass density	0.06 [Kg/m^2]
M_2/M_1	Ratio between RL and BM surface mass densities	$0.05M_1$
$K_1(x)$	BM stiffness	1.1 $10^{10}\exp(-2k_\omega x)$ [N/m]
$K_2(x)$	RL stiffness	$0.5K_1(x)$ [N/m]
$K_3(x)$	Internal BM-RL stiffness	$0.05K_1(x)$ [N/m]
$K_{nl}(x)$	Stiffness of the OHC active force	$500C_1(x)\omega_1{}^3/\omega_{bm}{}^2(x)$ [N/m]
$C_{nl}(x)$	Anti-damping coefficient of the OHC active force	0 [Ns/m]
$C_1(x)$	BM damping coefficient	1000exp(-$k_\omega x$) [Ns/m]
$C_2(x)$	RL damping coefficient	$5C_1(x)$ [Ns/m]
$C_3(x)$	Internal BM-RL damping coefficient	$2C_1(x)$ [Ns/m]
$\tau(x)$	OHC low-pass characteristic time	$0.13(\omega_1/\omega_{bm}(x))^{0.75}$ [ms]

g., the scale of the Greenwood map, the BM surface density, the length and height of the cochlear duct) are not dramatically different from those of several mammalian species. The viscosity coefficient is set to three times that of water to roughly schematize the additional viscous/viscoelatic losses within the elements of the OoC that are not included in the model. Among these structures, good candidates as sources of viscous damping are the compliant body of the OoC and the tectorial membrane. This consideration may help understanding why large values of the viscosity are sometimes necessary in this kind of models to get a better agreement with the observed phenomenology.

3. Results

The BM and RL velocity gain functions (amplitude normalized to the corresponding one at the cochlear base) are shown in Fig. 2, as a function of x, for a fixed frequency f_1 =12 kHz, along with the amplitude ratio and the phase difference between the RL and BM displacements, for three different values of the activity of the OHC force, $G = 0$ (black), $G =$ 0.5 (red), and $G = 1$ (blue), roughly corresponding to the response of a nonlinear model at three stimulus levels (very high, moderate, and near the hearing threshold). The effect of the RL motion on the TW generation is not included. Such a 2DOF model including focusing and viscous damping, with a suitable choice of the parameters, predicts gain dynamics of the RL motion larger than that of the BM at the lowest stimulus levels. The RL-BM amplitude ratio also increases in the peak region, approaching unity in this case. In this model, it is also possible to get an amplitude ratio exceeding unity, but this requires an unreasonably fine-tuned choice of the parameters across the auditory frequency range. The condition $|\mathrm{RL}|/|\mathrm{BM}| > 1$ was not strictly necessary in this study because its purpose was to show how to predict the effect of the RL contribution to the TW in a generic model that does not claim to reproduce a given experimental data set. The phase difference between RL and BM is weakly negative in the peak region in this particular model.

As shown in Fig. 3, with this particular parameter choice, adding the contribution of the RL motion to the generation of the TW complex wavenumber decreases the amplitude of the BM and RL response (thick black line) with respect to the corresponding model of Fig. 2, in which no RL effect was included (thin black line). This damping effect is due to the competition between a small increase of the real part of the wavenumber, which would boost focusing linearly (compressively in a nonlinear model), and a decrease of the imaginary part of it in the anti-damping region just before the peak (see bottom panels of Fig. 3). Even if the wavenumber is almost real-valued within the whole peak region in such 2-D viscous models (Sisto and Moleti, 2024), the variation of the relatively smaller imaginary part may have the largest impact on the response. This phenomenon may be better appreciated by artificially modifying the phase of the coefficient δ, which is partly equivalent to considering models in which the RL-BM phase difference is modified more consistently by finding suitable parameter settings. If an extra phase factor $e^{i\phi}$ is included in the factor δ, one may notice that the damping effect is compensated when the extra phase approximately cancels that of the RL-BM phase, (this happens for $\phi = 0.1$ rad in our simulation) while other phase shifts cause additional damping (negative shifts) or amplification (more positive shifts). The reason for this effect is

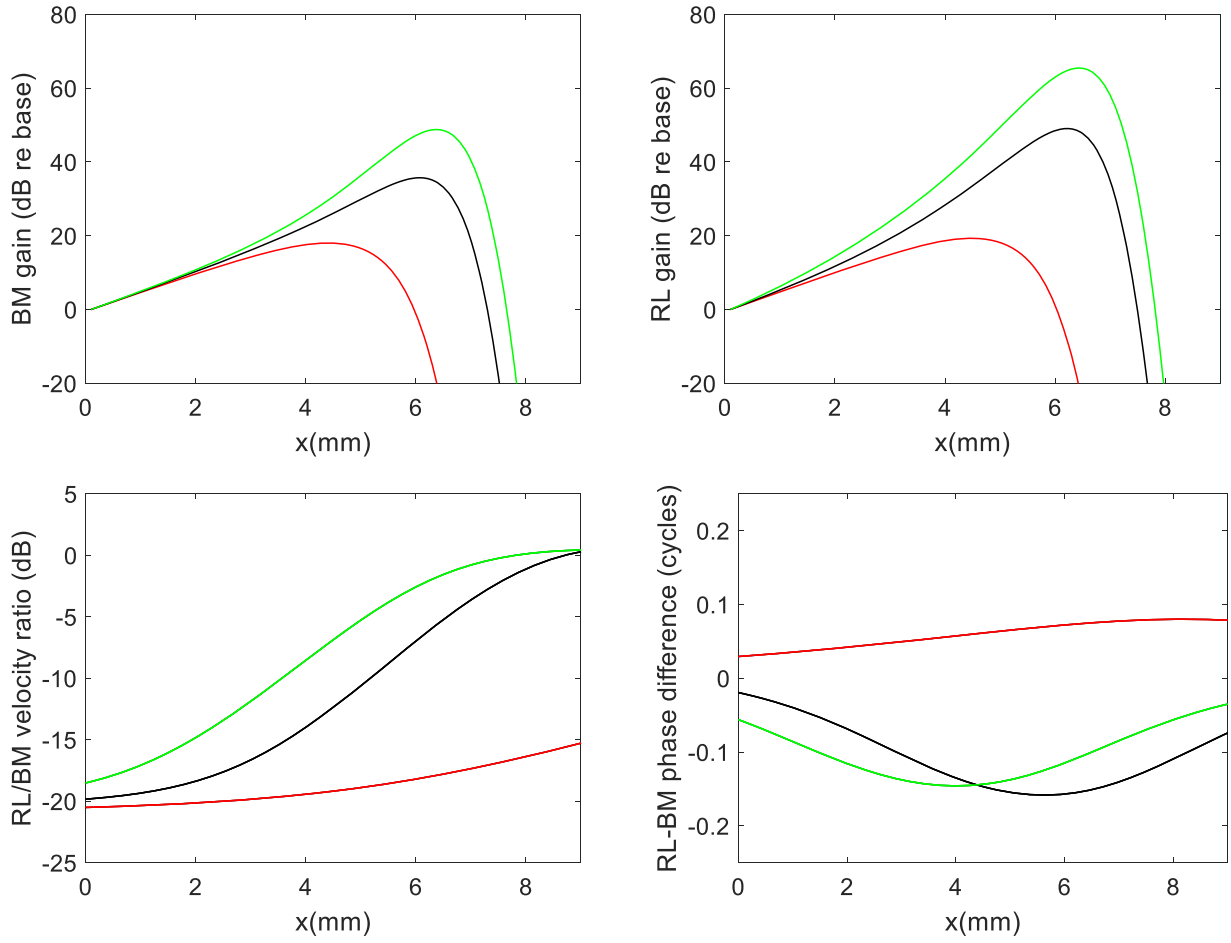

Fig. 2. Top: BM and RL velocity gain functions as a function of the longitudinal position x, for a frequency $f_1 = 12$ kHz, for three different strengths of the OHC mechanism, with $G = 0$, 0.5, 1 (red, black, green). The effect of the RL motion on the TW generation is not included. Bottom: Complex ratio between the RL and BM response (amplitude and phase) in the same model.

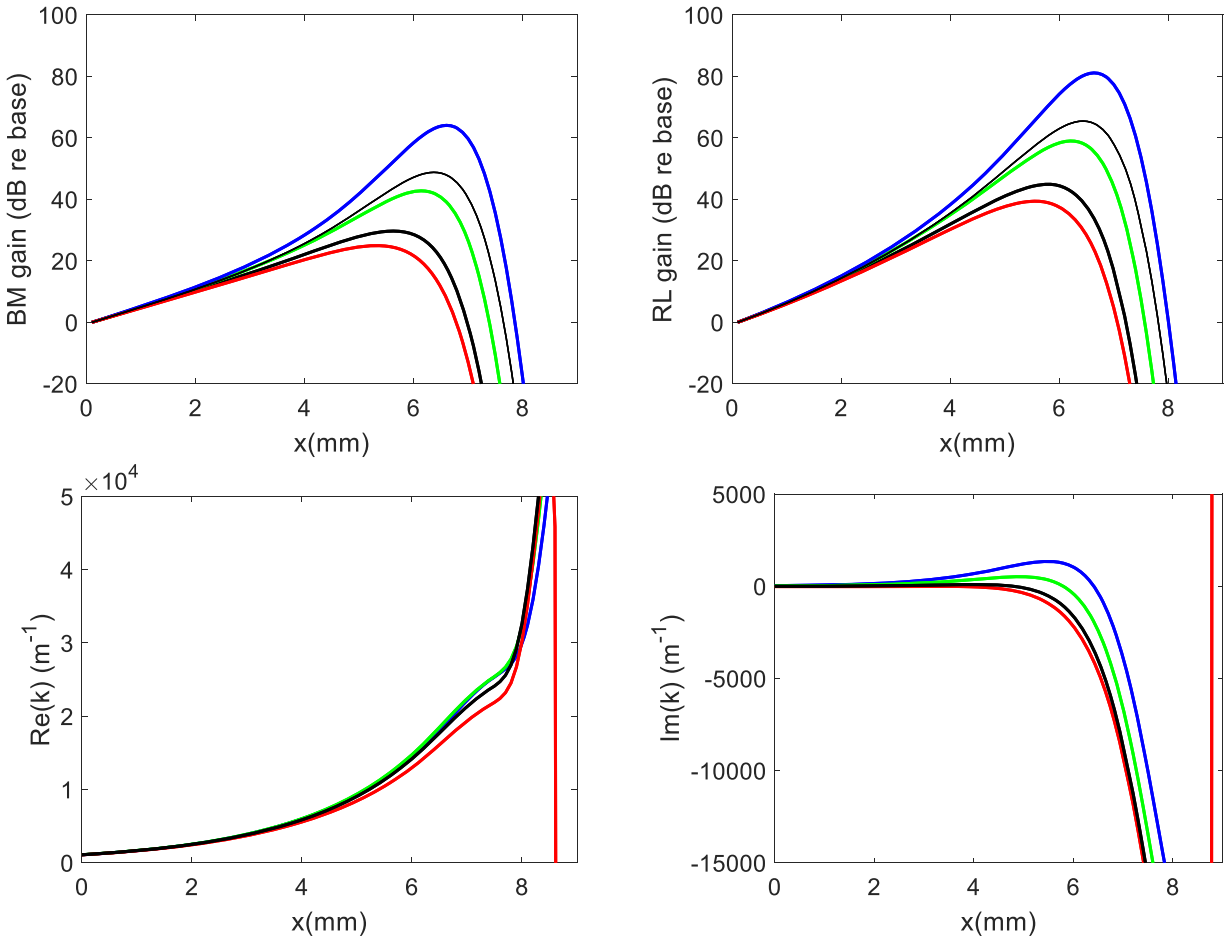

Fig. 3. Top: BM and RL velocity gain functions as a function of the longitudinal position x, for a frequency $f_1 = 12$ kHz, for $G = 1$, without the inclusion of the RL contribution to the TW (thin black line), with the RL contribution and no additional phase shift (thick black line), and with the RL contribution and an additional phase shift, $\phi = -0.1$ (red), $\phi = 0.1$ (green), and $\phi = 0.2$ rad (blue). Bottom: Real and imaginary part of the wavenumber for the same simulations.

evident from Eqs. (12–16). In a 2-D model dominated by focusing and viscosity the wavenumber is almost real (and the admittance imaginary) within the peak region (Sisto and Moleti, 2024). As a consequence, a weakly negative (positive) phase of the factor δ yields a negative (positive) real contribution to the wavenumber, i.e., a damping (antidamping) effect on the TW.

4. Discussion

If the RL and BM move in phase, the increase of the real part of the wavenumber is maximal. The amplification due to the internal active force tends to move the BM and the RL in phase opposition, while the external force applied to the two-mass system, the differential pressure, moves also its center of mass. Therefore, when the fluid focusing amplification is dominant over the active force, the contribution of the RL and BM sums up more coherently, making the mechanism more effective. At first sight, one could assume that the effect of this partly coherent sum should necessarily be that of increasing the BM and RL gain, but we have shown that the situation is more complex, because the (linear) effect of enhanced focusing associated with increasing the real part of the wavenumber could be overcome by the damping/antidamping (exponential) effect associated with modifying its imaginary part. In the 2-D WKB framework that we have used, the wavenumber is almost real-valued in the peak region, and in case of non-zero phase shift between RL and BM, the addition of the RL contribution would also add a small but significant imaginary part to the wavenumber. If the relative RL-BM phase is weakly positive (negative) an antidamping (damping) effect is predicted. This could be consistent with the monotonic decrease of the relative RL-BM phase generally observed by OCT experiments, approaching zero near the peak (Cho and Puria, 2022; Cooper et al., 2018; He et al., 2022; Lee et al., 2016; Strimbu et al., 2024; Olson et al., 2025). The theoretical observations of this study may suggest that the experimentally observed behavior of the RL-BM amplitude ratio and phase difference near the peak could be a necessary condition for the development of the peak itself. Indeed, a transition from an antidamping effect to a damping effect of the RL motion on the TW would occur where the RL is in phase with the BM. Therefore the RL-BM phase difference could be constrained to be relatively small within the peak region, or, equivalently, the peak position could be determined by such a condition, where the RL motion is dominant. On the other hand, it is worth noting that a small phase difference between the BM and RL motion is consistent with a dominant effect of focusing in the development of the peak gain, because the internal OHC force would tend to induce phase opposition.

Here, a caveat is necessary. In the WKB solution, the real part of the wavenumber is univocally associated with wave transmission and the imaginary part with exponential attenuation or amplification. In this particular model, the fast spatial variation of the wavenumber in the short-wave region may also weaken the main underlying assumption of the WKB approximation (spatial derivative of the wavenumber much smaller than the wavenumber squared). This is a serious issue, that involves, in general, such manipulations of the complex wavenumber. As we are iteratively modifying the relation between the wavenumber and the admittance by introducing the focusing factor α and a factor δ,

without changing the analytical form of the WKB solution, we cannot exclude the risk that the real and imaginary parts of the wavenumber partially mix in non-physical ways. If the manipulation is a relevant one, as in this case, the sensitivity of the solution to the introduction of complex terms in both α and δ should be carefully analyzed. A comparison with the predictions of a model solved with the FE method could help understanding the limitations of the WKB method, in this case and in others.

5. Conclusion

A 2-D cochlear model containing the full hydrodynamical coupling between the cochlear fluid and 2DOF mechanical elements, is presented and solved in the frequency domain in the WKB approximation. The OHC activity is modeled as an internal force between the BM and the RL. The low pass filtering associated with the slow build-up of the transmembrane potential of the OHC, acting as the source for the active actuator, provides an up-to-90° phase rotation, partially transforming an elastic force into an antidamping one.

The effect of including the deformation of the OoC in the equations for the propagation of the TW is computed in a particular realization of the model, in which the behavior of the RL-BM relative motion is not inconsistent with the experimental one (Cho and Puria, 2022; Cooper et al., 2018; He et al., 2022; Lee et al., 2016; Strimbu et al., 2024; Olson et al., 2025), obtaining, for a model in which the RL-BM phase difference is slightly negative, a reduction of the response amplitude with respect to the case in which the RL motion contribution is not considered. The results are analytically explained, by artificially modifying the RL-BM phase difference, suggesting that the behavior of the RL-BM relative phase observed by OCT experiments could be related to the position of the peak of the BM and RL response. We also emphasize the possible limitation of the WKB approach when applied to such problems in which the real and imaginary parts of the wavenumber play relevant and distinct roles, particularly in the case of rapidly varying wavenumbers.

CRediT authorship contribution statement

Renata Sisto: Writing – review & editing, Writing – original draft, Supervision, Software, Methodology, Investigation, Formal analysis, Conceptualization. **Arturo Moleti:** Writing – review & editing, Writing – original draft, Visualization, Methodology, Investigation, Formal analysis, Conceptualization.

Declaration of competing interest

Dear Editor,

The authors declare no competing interests about the manuscript: "Contribution of the Reticular Lamina motion to the traveling wave: a WKB approach".

Data availability

Data will be made available on request.

References

Cho, N.H., Puria, S., 2022. Cochlear motion across the reticular lamina implies that it is not a stiff plate. Sci. Rep. 12, 18715.

Cooper, N.P., Vavakou, A., van der Heijden, M., 2018. Vibration hotspots reveal longitudinal funneling of sound – evoked motion in the mammalian cochlea. Nat. Commun. 9, 3054.

He, W., Burwood, G., Porsov, E.V., et al., 2022. The reticular lamina and basilar membrane vibrations in the transverse direction in the basal turn of the living gerbil cochlea. Sci. Rep. 12, 19810.

Lee, H.Y., Raphael, P.D., Xia, A., Kim, J., Grillet, N., Applegate, B.E., Ellerbee Bowden, A. K., Oghalai, J.S, 2016. Two-dimensional cochlear micromechanics measured In vivo demonstrate radial tuning within the mouse organ of corti. J. Neurosci 36, 8160–8173.

Strimbu, C.E., Chiriboga, L.A., Frost, B.L., Olson, E.S., 2024. Regional differences in cochlear nonlinearity across the basal organ of Corti of gerbil: regional differences in cochlear nonlinearity. Hear. Res 443, 108951.

Olson, E.S., Dong, W., Applegate, B.E., Charaziak, K.K., Dewey, J.B., Frost, B.L., Meenderink, S.W.F., Nam, J.H., Oghalai, J.S., Puria, S., Ren, T., Strimbu, C.E., van der Heijden, M., 2025. Visualizing motions within the cochlea's organ of Corti and illuminating cochlear mechanics with optical coherence tomography. Hear. Res 455, 109154.

Altoè, A., Dewey, J.B., Chariaziak, K., Oghalai, J.S., CA, Shera, 2022. Overturning the mechanism of cochlear amplification via area deformation of the organ of Corti. J. Acoust. Soc. Am. 152, 2227.

Neely, S.T., Kim, D., 1986. A model for active elements in cochlear biomechanics. J. Acoust. Soc. Am. 79, 1472–1480.

Sisto, R., Shera, C.A., Altoè, A., Moleti, A., 2019. Constraints imposed by zero-crossing invariance on cochlear models with two mechanical degrees of freedom. J. Acoust. Soc. Am 146, 1685.

Zhou, W., Jabeen, T., Sabha, S., Becker, J., Nam, J.H., 2022. Deiters cells act as mechanical equalizers for outer hair cells. J. Neurosci 42, 8361–8372.

Samaras G., Meaud J. Compliant Deiters' Cells: a challenge for outer hair cell-based cochlear amplification?, Proceedings of the International Workshop on Mechanics of Hearing 2024, Ann Arbor, Michigan USA, 08-14 June 2024.

Steele, C.R., Taber, L.A., 1979 65. Comparison of WKB calculations and experimental results for three-dimensional cochlear models. J. Acoust. Soc. Am 1007.

Zweig, G., 1991. Finding the impedance of the organ of Corti. J. Acoust. Soc. Am 89, 1229–1254.

Frost BL Foundations of the Wentzel-Kramers-Brillouin approximation for models of cochlear mechanics in 1- and 2-D. J. Acoust. Soc. Am. 2024, 155, 358–379.

Shera, C.A., Tubis, A., Talmadge, C.L., 2005. Coherent reflection in a two-dimensional cochlea: short-wave versus long-wave scattering in the generation of reflection-source otoacoustic emissions. J. Acoust. Soc. Am 118, 287.

Shera, C.A., 2001. Intensity-invariance of fine time structure in basilar-membrane click responses: implications for cochlear mechanics. J. Acoust. Soc. Am 110, 332–348.

Nam, J.H., Fettiplace, R., 2012. Optimal electrical properties of outer hair cells ensure cochlear amplification. PLoS One 7, e50572.

Sisto, R., Moleti, A., 2021. Low-passed outer hair cell response and apical-basal transition in a nonlinear transmission-line cochlear model. J. Acoust. Soc. Am 149, 1296.

Sisto, R., Belardinelli, D., Moleti, A., 2021. Fluid focusing and viscosity allow high gain and stability of the cochlear response. J. Acoust. Soc. Am 150, 4283.

Sisto, R., Belardinelli, D., Altoè, A., Shera, C.A., Moleti, A., 2023. Crucial contributions of 3-D viscous hydrodynamics to cochlear amplification. J. Acoust. Soc. Am. 153, 77.

Lu, T.K., Zhak, S., Dallos, P., Sarpeshkar, R., 2006. Fast cochlear amplification with slow outer hair cells. Hear. Res 214, 45.

Duifhuis, H., 2012. Cochlear Mechanics: Introduction to a Time Domain Analysis of the Nonlinear Cochlea. Springer Science and Business Media, Berlin/Heidelberg, Germany.

Wang, Y., Steele, C.R., Puria, S., 2016. Cochlear outer-hair-cell power generation and viscous fluid loss. Sci. Rep 6, 19475.

Sisto, R., Moleti, A., 2024. The tonotopic cochlea puzzle: a resonant transmission line with a "non-resonant" response peak. JASA Exp. Lett 4, 074401.